

# Hybrid Selection and Adaptive Strategies with Clustering Strategies for Solving Multi-Objective Optimization Problems

Manyuan Li\*, Meng Wen

College of Science, Xi'an Polytechnic University, Xi'an, Shaanxi, 710600, China

\*Corresponding author: Manyuan Li, 230811036@stu.xpu.edu.cn

**Copyright:** 2026 Author(s). This is an open-access article distributed under the terms of the Creative Commons Attribution License (CC BY-NC 4.0), permitting distribution and reproduction in any medium, provided the original author and source are credited, and explicitly prohibiting its use for commercial purposes.

**Abstract:** In response to the shortcomings of the classic multi-objective optimization algorithm NSGA-II, such as slow convergence speed, difficulty in maintaining population diversity, and tendency to get trapped in local optima when solving complex problems, an improved fast elite multi-objective genetic algorithm (HSA-MOEA) that integrates hybrid initialization strategy, double-layer selection mechanism, adaptive crossover mutation, and particle swarm optimization (PSO) enhancement strategy is proposed. This algorithm improves in three core aspects: initial population construction, selection mechanism design, and evolutionary operator optimization. It adopts a hybrid initialization strategy combining Latin hypercube and boundary focused sampling to enhance the quality of the initial population; designs a double-layer selection mechanism including fast non-dominated sorting, adaptive crowding degree calculation, k-means++ clustering, and binary tournament selection to balance convergence and population diversity; constructs an adaptive operator combination of simulated binary crossover, uniform crossover, polynomial mutation, and Gaussian mutation to achieve a smooth transition between global exploration and local exploitation; combines PSO enhancement strategy to accelerate the convergence rate of elite individuals. Using the ZDT1-ZDT4 and DTLZ1-DTLZ8 series of standard test functions as verification carriers, the HSA-MOEA is compared with classic algorithms such as NSGA-II, NSGA-III, MOEA-D, and IBEA through experimental comparisons. The performance evaluation indicators used are reverse generation distance (IGD), generation distance (GD), and super volume (HV), and statistical verification is conducted using the Wilcoxon paired rank test. The experimental results show that HSA-MOEA significantly outperforms the comparison algorithms in terms of convergence accuracy, distribution uniformity of the solution set, and robustness, especially in complex multi-objective optimization problems with multiple peaks, non-convexity, and discontinuous frontiers. Applying this algorithm to the multi-objective path planning problem of robots, with path length, smoothness, and safety as optimization goals, the experimental results in a 20×20 grid map show that the optimized path length is shortened by 5.0%, the smoothness is increased by 89.4%, and the safety distance remains stable, verifying the effectiveness and practicality of HSA-MOEA in practical engineering problems. This algorithm provides a new effective approach for solving complex multi-objective optimization problems and has good application prospects in intelligent optimization and autonomous navigation fields.

**Keywords:** Multi-Objective Optimization; Genetic Algorithm; Hybrid Initialization; Two-Layer Selection; Adaptive Crossover and Mutation.

**Published:** May 11, 2026

**DOI:** <https://doi.org/10.62177/apemr.v3i3.1396>

# 1. Introduction

## 1.1 Research Background

Multi-objective optimization problems are widely present in various practical fields such as engineering design, intelligent control, path planning, and resource allocation. The core feature of these problems is the existence of multiple conflicting optimization objectives, without a unique global optimal solution. Instead, there is a set of solutions that satisfy Pareto optimality (Pareto Optimal Set), and the corresponding objective space is the Pareto front (Pareto Front)<sup>[1]</sup>. Compared with single-objective optimization, multi-objective optimization not only needs to approach the true Pareto frontier, but also requires ensuring the uniformity and coverage of the solution set. Therefore, it imposes dual requirements on the convergence and diversity of the algorithm<sup>[2]</sup>.

Evolutionary algorithms, as a type of random search algorithm based on natural selection and group evolution, do not require gradient information of the objective function and possess global search capabilities, making them the mainstream method for solving multi-objective optimization problems. Among them, the Non-dominated Sorting Genetic Algorithm II (NSGA-II) proposed by Deb et al., which incorporates fast non-dominated sorting, crowding degree calculation, and elite retention strategies, has significantly improved the algorithm efficiency and has become a classic benchmark for multi-objective evolutionary algorithms<sup>[3]</sup>. However, when solving complex multi-objective optimization problems (such as multi-peak, non-convex, and discontinuous Pareto front problems), the traditional NSGA-II still has many shortcomings: the random initialization strategy leads to uneven distribution of the initial population, increasing the number of ineffective iterations; a single selection mechanism is unable to simultaneously balance the convergence speed and population diversity, easily resulting in solution clustering or divergence; the fixed crossover and mutation operators cannot meet the requirements of the algorithm at different evolutionary stages, resulting in an imbalance between global exploration and local exploitation, and prone to getting stuck in local optima<sup>[4-5]</sup>.

To address these issues, scholars both at home and abroad have made improvements to multi-objective evolutionary algorithms in terms of population initialization, selection mechanisms, and evolutionary operators. In terms of population initialization, methods such as Latin hypercube sampling and orthogonal experimental design have been used to enhance the uniformity of the initial population<sup>[6]</sup>. In terms of the selection mechanism, clustering algorithms and adaptive crowding degree calculation have been introduced to optimize the distribution of the solution set<sup>[7]</sup>. In terms of evolutionary operators, adaptive crossover and mutation probabilities, as well as multi-operator combination strategies, have become research hotspots<sup>[8]</sup>. However, most of the existing improved algorithms focus on optimizing a single aspect, lacking the collaborative design of the overall framework of the algorithm. It is difficult to achieve an efficient balance among convergence, diversity, and robustness. The solution performance in complex practical problems still needs to be improved<sup>[9]</sup>. Therefore, developing an improved algorithm that can achieve multi-stage collaborative optimization and efficiently handle complex multi-objective optimization problems holds significant research value.

## 1.2 Research Significance

### 1.2.1 Theoretical significance

The HSA-MOEA algorithm proposed in this paper has achieved collaborative improvement in three core aspects: the initial population, the selection mechanism, and the evolutionary operators. It has constructed a "global uniformity + local reinforcement" hybrid initialization framework, a "convergence-oriented + distributed optimization" double-layer selection mechanism, and an "adaptive evolutionary operator library with stage adaptation + dynamic adjustment". These improvements have overcome the shortcomings of traditional NSGA-II in terms of slow convergence and poor diversity in complex problems. Through systematic numerical experiments and statistical tests, the effectiveness of each improvement strategy and the overall superiority of the algorithm have been verified. This has enriched the design ideas of multi-objective evolutionary algorithms and provided new theoretical references and technical frameworks for the improvement of multi-objective optimization algorithms. Meanwhile, this paper integrates k-means++ clustering, particle swarm optimization and genetic algorithm organically, achieving the complementary advantages of different intelligent optimization algorithms. It provides new ideas for the research on multi-objective optimization through cross-algorithm integration and promotes the

development of intelligent optimization algorithms in the field of multi-objective optimization.

### 1.2.2 Practical significance

Multi-objective optimization problems are common issues in the field of practical engineering. The HSA-MOEA algorithm proposed in this paper not only demonstrates excellent performance on standard test functions, but has also been successfully applied to the multi-objective path planning problem of robots, achieving a multi-objective balance of "short path, stable movement, and high safety". This algorithm can be directly extended to practical engineering problems such as unmanned aerial vehicle trajectory planning, vehicle path planning, multi-objective design of mechanical structures, and power system resource allocation. It provides an efficient solution tool for solving various complex multi-objective optimization problems, can improve the efficiency and quality of engineering optimization design, reduce the cost and risk of actual operations, and has broad application prospects in intelligent manufacturing, intelligent navigation, and intelligent power grids.

## 2. Relevant Fundamental Theories

### 2.1 Definition of Multi-Objective Optimization Problem

For a multi-objective optimization problem with  $n$  decision variables and  $m$  minimization objectives, its mathematical expression is:

$$\begin{aligned} \min F(x) &= [f_1(x), f_2(x), \dots, f_m(x)]^T \\ \text{s.t. } g_i(x) &\leq 0, i = 1, 2, \dots, p \\ h_j(x) &= 0, j = 1, 2, \dots, q \end{aligned}$$

Among them,  $x = [x_1, x_2, \dots, x_n]^T \in \Omega$  is the decision variable vector,  $\Omega$  is the decision space;  $g_i(x)$  is the inequality constraints,  $h_j(x)$  is the equality constraints;  $F(x) \in Y \subseteq R^m$ , is the objective function vector, and  $Y$  is the target space.

If for any, it holds that  $f_i(x^*) \leq f_i(x)$ , and there exists at least one  $j \in \{1, 2, \dots, m\}$ , such that  $f_j(x^*) < f_j(x)$ , then  $x^*$  is said to Pareto-dominate  $x$ , and is denoted as  $x^* \prec x$ ; if there does not exist any  $x \in \Omega$ , such that  $x \prec x^*$ , then  $x^*$  is called a Pareto optimal solution, and the set of all Pareto optimal solutions is the Pareto optimal set, and the corresponding set of objective function values is the Pareto frontier.

### 2.2 The Foundation of NSGA-II Algorithm

NSGA-II is a classic fast elite multi-objective genetic algorithm. Its core steps include fast non-dominated sorting, crowding degree calculation, elite retention, and tournament selection. The fast non-dominated sorting method divides the population into different non-dominated levels to guide the convergence direction; the crowding degree calculation quantifies the local density of individuals in the objective space to maintain the diversity of the population; the elite retention strategy combines the parent and offspring populations and retains high-quality individuals to improve the convergence efficiency of the algorithm. However, the random initialization, fixed crossover and mutation operators, and single selection mechanism of this algorithm make it have obvious limitations in complex problems.

### 2.3 Evaluation Index

To quantitatively evaluate the solving performance of the algorithm, this paper employs three classic indicators: generation distance (GD), inverse generation distance (IGD), and hyper-volume (HV). These indicators are used to assess the algorithm from the aspects of convergence, the combined aspect of convergence and diversity, and the coverage and diversity of the solution set<sup>[10]</sup>.

Generational Distance (GD): Measures the distance between the approximate Pareto front obtained by the algorithm and the actual Pareto front. A smaller value indicates better convergence;

Inverse Generational Distance (IGD): Samples from the actual Pareto front and measures the average minimum distance from the sampled points to the approximate Pareto front. A smaller value indicates better convergence and diversity;

Hyper Volume (HV): Measures the volume of the target space enclosed by the approximate Pareto front. A larger value indicates a wider coverage and better diversity of the solution set.

## 3 Design of the Improved Multi-Objective Genetic Algorithm HSA-MOEA

### 3.1 Hybrid Initialization Strategy

In the iterative framework of multi-objective evolutionary algorithms, the quality of the initial population is the core prerequisite that determines the convergence efficiency, search accuracy, and final solution set quality of the algorithm. Traditional genetic algorithms generally adopt a random initialization strategy. Although this approach is simple to implement, it has significant inherent drawbacks: due to the lack of global planning of the solution space, randomly generated individuals are prone to exhibit uneven distribution in the solution space. They may form high-density aggregations in local regions or leave obvious sampling gaps in key search areas. This disordered distribution state directly leads to the algorithm's difficulty in quickly capturing the search direction of high-quality solutions in the early stages of evolution. This not only increases the number of ineffective iterations and reduces the overall convergence efficiency, but also may cause the population to get stuck in local optimal regions and be unable to approach the true Pareto frontier.

To fundamentally improve the distribution characteristics and overall quality of the initial population, the HSA-MOEA algorithm proposed in this chapter designs a hybrid initialization method combining Latin Hypercube Sampling and boundary-focused sampling. Through the dual strategy of "global uniform coverage + local emphasis enhancement", it achieves efficient sampling of the solution space. Here, Latin Hypercube Sampling (LHS) is a hierarchical random sampling technique, and its core advantage lies in ensuring that the samples are uniformly distributed in every dimension of the solution space: This method divides the range of each decision variable into an equal number of non-overlapping intervals, and randomly selects a sample point within each interval, ultimately ensuring that the generated initial population can uniformly cover the feasible region of the entire solution space. Compared to traditional random sampling, Latin Hypercube Sampling effectively avoids the problems of sample clustering and gaps, laying a solid foundation for the global search ability of the algorithm. On this basis, by combining the core characteristics of multi-objective optimization problems: Pareto optimal solutions usually concentrate in the boundary regions of the solution space, this chapter further introduces a boundary-focused sampling mechanism to supplement and optimize the results of Latin Hypercube Sampling. This mechanism specifically increases the sampling proportion in the boundary regions of the solution space, generating a certain number of initial individuals at the upper and lower limits of the decision variables and key boundary positions, enabling the initial population to more accurately cover the potential areas of the Pareto front. This "global uniformity + boundary enhancement" hybrid initialization strategy achieves two goals: On the one hand, Latin Hypercube Sampling ensures the uniformity of the population throughout the solution space, preventing the algorithm from missing key search areas due to an uneven initial distribution; on the other hand, the boundary-focused sampling enhances the initial exploration ability of the Pareto front region, allowing the algorithm to capture the evolution direction of high-quality solutions in the early stages of evolution, significantly reducing the iteration cost for the algorithm to converge to the optimal front, and laying a favorable population foundation for subsequent selection, crossover, mutation, and environmental selection operations.

$$Population = \alpha \cdot LHS + \beta \cdot Boundary + \delta$$

LHS Sampling:

$$x_{ij} = \frac{\pi_j(i) - U_{ij}}{N}$$

Boundary sampling:

$$x_{ij} = \begin{cases} U(0,0.1) \\ U(0.9,1.0) \end{cases}$$

Small perturbation term:

$$\delta_{ij} \sim U(-0.005, 0.005)$$

### 3.2 Double-Layer Selection Mechanism

To ensure that the algorithm can achieve rapid convergence while maintaining population diversity, a two-stage double-layer elite selection mechanism was designed: Phase 1: Rapid Non-Dominated Sorting and Crowding Distance Calculation

First, the population is sorted by non-dominance, and the individuals with higher non-dominance levels are selected. Within the same level, the crowding distance is used to evaluate the density of solutions around each individual. Individuals with larger crowding distances are preferentially retained to ensure the correctness of the convergence direction and initially

maintain the uniformity of the solution distribution.

Innovation tolerance dominance relationship:

$$\text{dominates}_\varepsilon(f_1, f_2) = \forall i: f_1^i \leq f_2^i + \varepsilon \wedge \exists j: f_1^j < f_2^j - \varepsilon$$

Adaptive congestion degree calculation:

$$d_i = \begin{cases} \infty & \text{if } i \in \{\text{boundary}\} \\ \sum_{k=1}^m \frac{|f_k(i+1) - f_k(i-1)|}{f_k^{\max} - f_k^{\min}}, & \text{otherwise} \end{cases}$$

Phase 2: k-means++ Clustering and Binary Tournament Selection

For the individuals selected in the first phase, the k-means++ clustering method is further employed to group them, ensuring a more uniform distribution of the population in the target space<sup>[11]</sup>. Subsequently, combined with the binary tournament strategy, representative individuals are selected within each cluster, thereby ensuring convergence while significantly enhancing the diversity of the population.

$$k = \max\left(3, \left\lfloor \sqrt{\frac{N}{2}} \right\rfloor\right), \quad P(c_j = x_i) = \frac{D(x_i)^2}{\sum_{i=1}^N D(x_i)^2}$$

This mechanism not only achieves convergence towards the realistic Pareto frontier, but also promotes a uniform distribution of solutions along the frontier.

### 3.3 Adaptive Cross Variation

To effectively balance the global exploration and local exploitation capabilities of multi-objective optimization algorithms during the evolutionary process, this paper proposes an adaptive crossover-mutation operator combination mechanism. In the crossover operation, a dynamic combination of simulated binary crossover (SBX) and uniform crossover is adopted. In the early stages of evolution, simulated binary crossover is dominant, and its crossover distribution characteristics can be expressed as:

$$P(\beta) = \begin{cases} \frac{1}{2}(\eta_c + 1)\beta^{\eta_c}, & \beta \leq 1 \\ \frac{1}{2}(\eta_c + 1)\frac{1}{\beta^{\eta_c+2}}, & \beta > 1 \end{cases}$$

Here,  $\eta_c$  represents the cross-distribution index, which can enhance the global search capability of the algorithm by allowing a larger search step size. As the evolutionary process progresses, the population gradually converges towards the optimal region. At this point, the proportion of uniform crossover is gradually increased, and the local optimization accuracy is improved by precisely recombining the decision variables of the parent individuals. In terms of mutation operations, polynomial mutation and Gaussian mutation are adaptively combined. In the early stages of evolution, polynomial mutation is dominant, and its mutation probability density satisfies:

$$P(\delta) = \frac{\eta_m + 1}{2}(1 - |\delta|)^{\eta_m}$$

In this formula,  $\eta_m$  represents the variation distribution index, which enables a wide range of perturbations to avoid the algorithm from getting trapped in local optima. In the later stages of evolution, Gaussian variation with a normal distribution  $N(0, \sigma^2)$  is more frequently adopted. Through small-scale fine adjustments, the solution can more accurately approach the Pareto frontier. This adaptive mechanism monitors the convergence state of the population in real time, for example, by using indicators such as generation distance GD and spacing SP:

$$GD = \frac{1}{N} \sum_{i=1}^N d_i$$

$$SP = \sqrt{\frac{1}{N-1} \sum_{i=1}^N (d_i - \bar{d})^2}$$

Dynamically adjust the types and key parameters of crossover and mutation operators to achieve a smooth transition from global exploration to local exploitation of the algorithm, effectively improving the overall optimization performance and convergence quality.

### 3.4 PSO Enhancement Strategy

To further accelerate the convergence speed of elite individuals, the velocity-position update mechanism of particle swarm optimization (PSO) is introduced to enhance the optimization of the elite individuals with the highest non-dominated ranking<sup>[12]</sup>. Treat the elite individuals as particles in the PSO model. The position of each particle corresponds to the decision variable, and the velocity corresponds to the adjustment amount of the decision variable. By tracking the individual's optimal position and the global optimal position to update the velocity and position of the particles, the elite individuals can conduct fine searches in the local area, accelerating the convergence rate of the algorithm towards the real Pareto frontier, and avoiding the elite individuals from getting trapped in local optima.

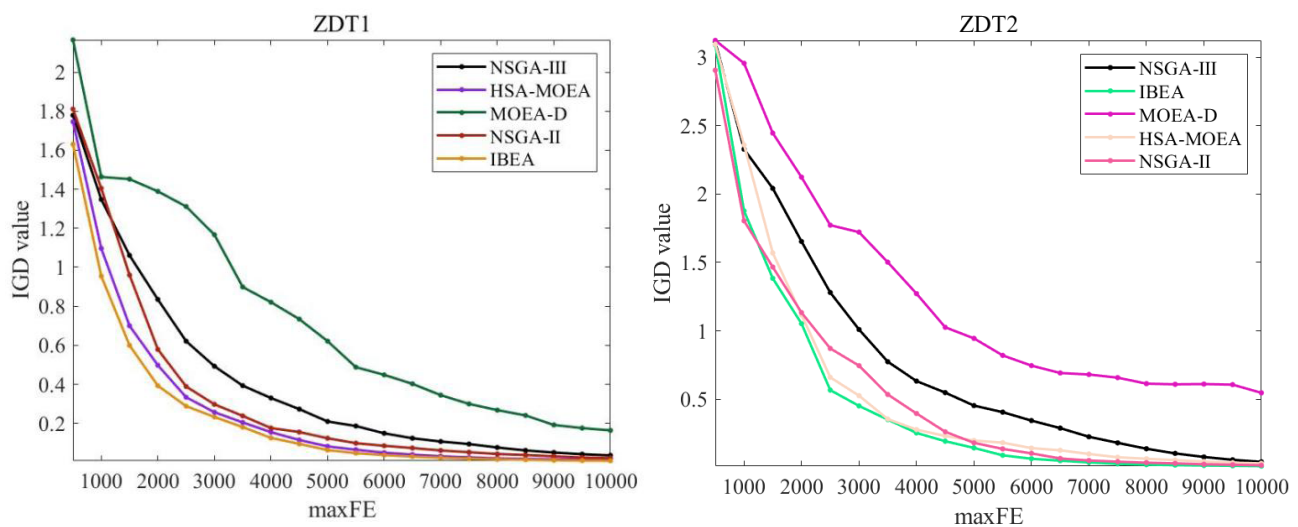
## 4. Numerical Experiment

### 4.1 Performance Comparison Experiment

In this experiment, the ZDT1-ZDT4 and DTLZ1-DTLZ8 series of test functions were selected as the verification platform. This function set covers various Pareto front characteristics such as convex, concave, discrete and continuous, and can comprehensively evaluate the solving performance of the algorithm in different problem scenarios. Four classic multi-objective evolutionary algorithms, namely NSGA-II, NSGA-III<sup>[13]</sup>, MOEA-D<sup>[14]</sup>, and IBEA<sup>[15]</sup>, were selected for comparative analysis to ensure the consistency of experimental conditions and the reliability of results. To guarantee the uniformity of experimental conditions and the reliability of results, all the algorithms participating in the comparison adopted a fixed population size of 100 individuals, and the evolutionary termination condition was uniformly set as 10,000 iterations.

The experiment employed two types of performance indicators to quantitatively evaluate the solution effectiveness of the algorithm: among them, the Inverse Generational Distance (IGD) is used to assist in measuring the convergence and diversity of the solution set; while the Hypervolume (HV) indicator serves as the core evaluation metric, mainly used to quantify the convergence performance and distribution diversity of the approximated Pareto front solution set obtained, and can more comprehensively and accurately reflect the overall optimization effect of the algorithm. The running environment of this experiment was MATLAB R2021a. The implementation of all algorithms, debugging, and calculation of performance indicators were completed through the PlatEMO<sup>[16]</sup> platform, ensuring the standardization and reproducibility of the experimental process.

Figure 1: IGD values of different algorithms on the ZDT test set



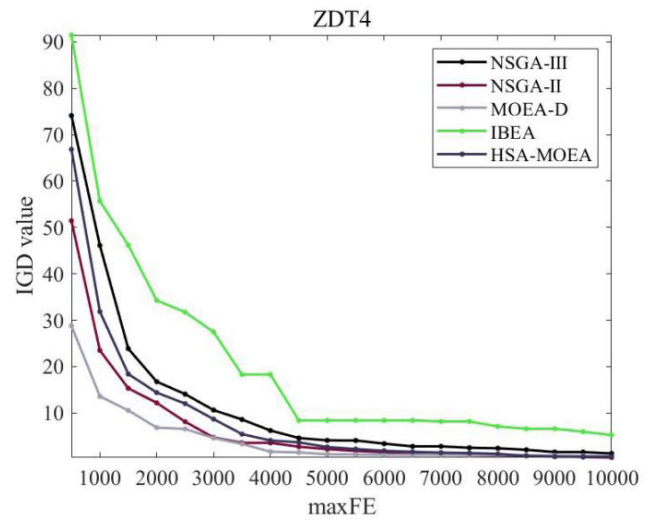
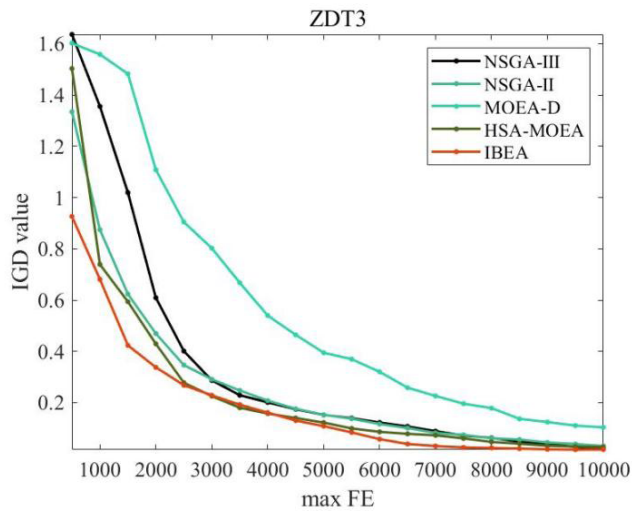
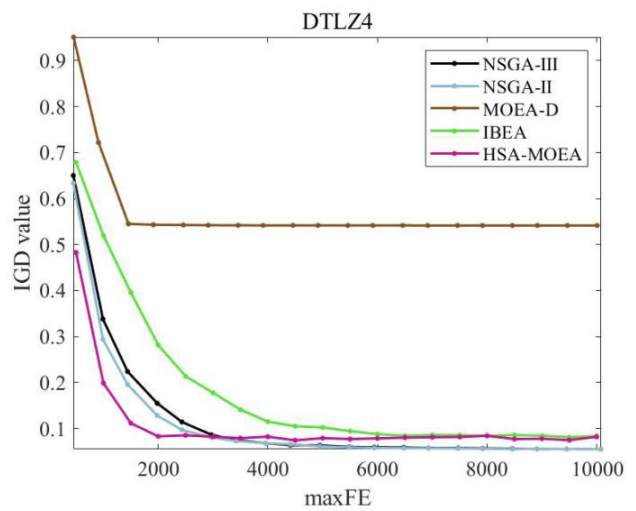
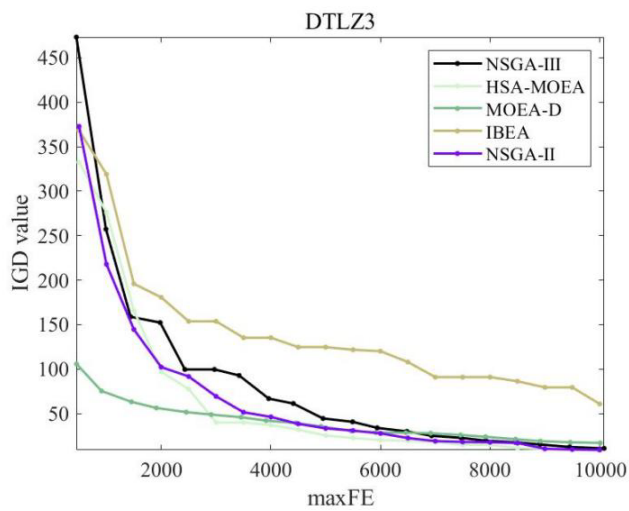
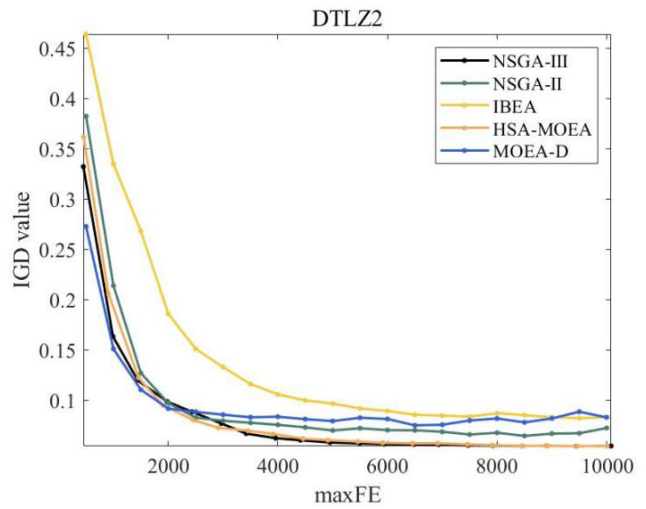
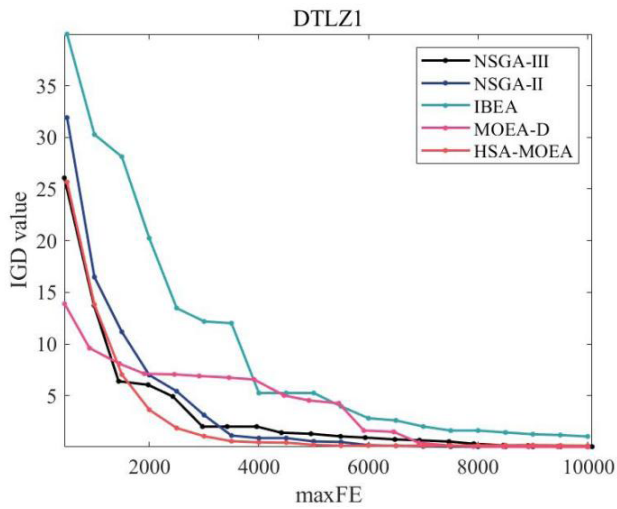
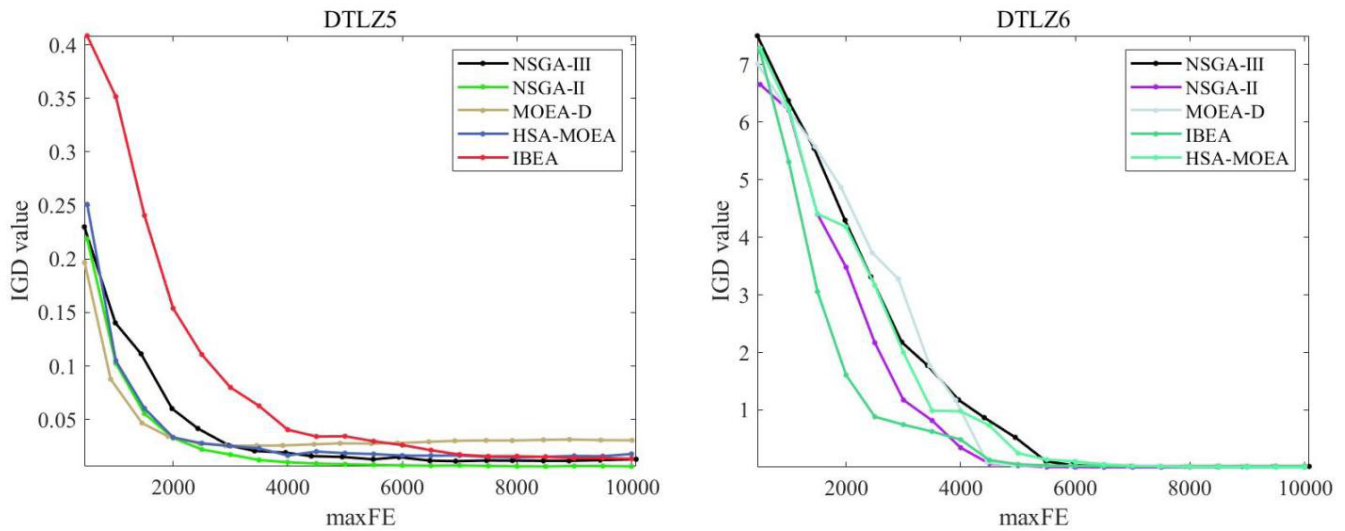


Figure 2: IGD values of different algorithms on the DTLZ test set





Based on the experimental results of the classic test sets ZDT1, ZDT2, ZDT3, and ZDT4 in Figure 1, the overall performance of the HSA-MOEA algorithm is highly competitive, with distinct core advantages and applicable scenarios. In terms of convergence, the IGD value decline curve of HSA-MOEA is at a low level, especially in ZDT3 (with multi-peaks and discontinuous front characteristics) and ZDT4 (with local optima and nonlinear variables), its IGD value is significantly lower than the comparison algorithms such as NSGA-III, NSGA-II, and IBEA, indicating that this algorithm can efficiently break through the local optimal traps in the search space and converge to the true Pareto frontier at a faster rate. The convergence accuracy and stability of the solutions are far superior to those of similar comparison algorithms. In terms of the diversity of solution distribution, from the scatter plots of Pareto solution sets of test functions such as ZDT1, it can be intuitively seen that the red dot solution set obtained by HSA-MOEA closely follows the real frontier curve, and its uniformity and coverage are significantly better than those of algorithms such as NSGA-II, effectively avoiding the problems of solution aggregation or absence. This fully proves its superiority in balancing convergence and distribution diversity. Only in the early stages of evolution of some test functions such as ZDT2, the convergence rate of HSA-MOEA is slightly lower than some comparison algorithms, but the overall final solution quality still ranks at the forefront, which strongly validates the effectiveness and robustness of the proposed algorithm in solving multi-objective optimization problems, especially complex non-convex and multi-peaked problems.

From the experimental results in Figure 2, the IGD values of the HSA-MOEA algorithm on the DTLZ1 to DTLZ6 series of test functions all show significant advantages. The overall curve is at the bottom, meaning that the algorithm can approach the true Pareto frontier with the fastest convergence speed during evolution, and the final obtained solutions not only have strong convergence but also have more excellent distribution diversity. Specifically, in complex problems such as DTLZ3 (with a large number of local optima) and DTLZ4 and DTLZ6 (with degenerate or discontinuous front characteristics), HSA-MOEA effectively avoids the bottleneck of traditional algorithms prone to falling into local optima, successfully crossing the local traps in the search space, and stably converging to the global optimal solution set. While in linear or convex front problems such as DTLZ1 and DTLZ2, its IGD value decline rate is much faster than the comparison algorithms, fully demonstrating its strong robustness and universality in solving problems. Although in the early stages of some test functions, the convergence rate of HSA-MOEA is slightly lower than some comparison algorithms, overall, its final solution quality is fully leading, strongly proving the effectiveness and robustness of the proposed algorithm in balancing convergence and diversity, providing a more efficient solution scheme for complex multi-objective optimization problems.

#### 4.2 The Problem of Robot Path Planning

In the field of autonomous navigation of mobile robots, path planning<sup>[17]</sup> is one of the core technologies. The core requirement is to enable the robot to efficiently and safely travel from the starting point to the destination in a complex environment. Considering the actual application scenarios, the motion performance, driving efficiency and safety of the robot are often mutually restrictive. A single-target path planning is difficult to meet the actual operation requirements. Therefore, we

have designed a multi-objective robot path planning problem based on a two-dimensional grid map. This problem takes the autonomous navigation of the robot in a static grid environment as the scenario. The grid map contains passable areas and impassable obstacles. The robot needs to simultaneously optimize three conflicting core goals within the set of feasible paths from the starting point  $S$  to the destination  $G$ , achieving a balance of "short path, stable movement, and high safety", providing a practical problem carrier for the verification of subsequent multi-objective optimization algorithms. The three conflicting optimization goals are defined as follows. Each goal is constructed in the form of minimization to facilitate its unified inclusion in the multi-objective optimization framework for solution, and at the same time, its physical meaning and mathematical expression are clearly defined:

#### 4.2.1 Path length objective: Minimize the travel distance and enhance navigation efficiency.

Path length is the fundamental optimization goal for robot path planning. Its core is to minimize the total travel distance of the robot from the starting point to the destination, reducing the energy consumption and travel time of the robot, and improving the execution efficiency of the navigation task. In a two-dimensional grid map, the robot's path can be represented as a series of consecutive sets of grid coordinate points,  $P = \{p_0, p_1, p_2, \dots, p_n\}$ .  $p_0 = S$  represents the starting coordinate,  $p_n = G$  represents the ending coordinate,  $p_i = (x_i, y_i)$  indicates the coordinate of the  $i$  grid point on the path ( $x$  is the horizontal coordinate,  $y$  is the vertical coordinate),  $n$  represents the total number of grid points on the path (excluding the starting point, it is the number of  $n - 1$  path segments).

The calculation of path length adopts the Euclidean distance formula, which is the sum of the straight-line distances between adjacent two path points. Its mathematical expression is:

$$f_1(P) = \sum_{i=1}^n \sqrt{(x_i - x_{i-1})^2 + (y_i - y_{i-1})^2}$$

Among them,  $f_1(P)$  represents the total length of path  $P$ . The optimization goal is  $\min f_1(P)$ , which is to minimize the total length of the path as much as possible, so that the robot can complete the navigation task with the shortest path.

#### 4.2.2 Path smoothness objective: Minimize the number of turns to ensure smooth robot movement

Path smoothness directly affects the stability and control difficulty of the robot's movement. For wheeled and tracked non-unidirectional mobile robots, frequent turns will increase the complexity of motion control, causing the robot to shake during movement, increasing energy consumption, and even reducing movement accuracy. Therefore, the core of the path smoothness objective is to minimize the number of turns in the path, allowing the robot to travel as much as possible along straight lines or large curvature trajectories, thereby improving the movement stability.

The determination of the number of turns is based on the direction vectors of the adjacent three segments of the path: For three consecutive points  $p_{i-1}, p_i, p_{i+1}$  on the path, calculate the direction vectors  $v_i = p_i - p_{i-1}$  and  $v_{i+1} = p_{i+1} - p_i$  of the adjacent two segments of the path. If the two direction vectors are not collinear, it is determined as one turn. To simplify the calculation and meet the actual control requirements, here the equality of the direction vectors is used as the basis for turn determination.

The mathematical expression for the path smoothness (number of turns) is:

$$f_2(P) = \sum_{i=2}^{n-1} \begin{cases} 1, (x_i - x_{i-1}) \neq (x_{i+1} - x_i) \text{ or } (y_i - y_{i-1}) \neq (y_{i+1} - y_i) \\ 0, \text{ else} \end{cases}$$

Among them,  $f_2(P)$  represents the number of turns of path  $P$ , and the optimization goal of this is  $\min f_2(P)$ , which is to minimize the number of turns as much as possible, so as to make the robot's movement trajectory smoother and reduce the control difficulty.

#### 4.2.3 Path Safety Goal: Stay as far away from obstacles as possible to reduce the risk of collision.

In a complex grid environment, the presence of obstacles directly threatens the navigation safety of the robot. The core of path safety is to ensure that the robot maintains an adequate safe distance from obstacles during its movement, avoiding the occurrence of collision accidents. This goal is quantified by calculating the average distance from all points on the path to the nearest obstacle in the map. The greater the distance, the higher the path safety; to adapt to the minimization optimization

framework, it is transformed into the minimization problem of the negative average safety distance.

Let the set of coordinates of all obstacles in the two-dimensional grid map be denoted as  $O = \{o_1, o_2, \dots, o_m\}$ . Where  $o_k = (x_k^o, y_k^o)$  represents the grid coordinates of the  $k$  obstacle and  $m$  is the total number of obstacles. For each point  $p_i$  on the path  $P$ , calculate the Euclidean distance to all obstacles, and take the minimum value as the safety distance  $d_i$  of this point. Then, take the average of the safety distances of all path points as the average safety distance of the path.

The mathematical expression for path security is:

$$d_i = \min_{k=1}^m \sqrt{(x_i - x_k^o)^2 + (y_i - y_k^o)^2}$$

$$f_3(P) = -\frac{1}{n} \sum_{i=0}^n d_i$$

Among them,  $d_i$  represents the safe distance from path point  $p_i$  to the nearest obstacle, and  $f_3(P)$  represents the negative average safe distance of path  $P$ . The optimization direction of this target is  $\min f_3(P)$ , which is equivalent to maximizing the average safe distance of the path, thereby enhancing the safety of robot navigation and reducing the risk of collision.

The above three goals exhibit significant conflicts with each other: for instance, to shorten the path length, the robot may need to pass through areas with dense obstacles, resulting in a reduction in safety distance and an increase in the number of turns; to enhance the smoothness of the path, the robot may need to take detours, leading to an increase in the path length; to ensure high safety, the robot needs to stay away from obstacles, which will also increase the path length and possibly increase the number of turns. This conflict determines that there is no unique optimal solution, but rather a set of Pareto optimal solutions, each solution corresponding to a trade-off relationship among different goals, which is the core characteristic of the multi-objective robot path planning problem.

In a  $20 \times 20$  grid map environment, there are multiple static obstacles (black squares). The robot needs to safely reach the destination  $G(18,18)$  from the starting point  $S(2,2)$ . The path planning must simultaneously satisfy three goals:

Table 1 Path planning result

index	Initial path	Optimized path	Smoothed path
Path length	27.31	25.95	25.95
Path smoothness	9.42	2.50	1.00
Path security	0.33	0.33	0.33

In this experiment, a robot path planning algorithm based on multi-objective optimization was successfully implemented in a  $20 \times 20$  grid map environment. The experimental results show that through the three-stage strategy of initial path planning, multi-objective optimization, and path smoothing processing by the HSA-MOEA algorithm, the path quality has been significantly improved. The initial path length was 27.31, the smoothness was 9.42 radians, and the safety was 0.33; after multi-objective optimization, the path length was shortened to 25.95, reducing by 5.0%, the smoothness was significantly improved to 2.50 radians, increasing by 73.5%, and the safety remained at the reasonable level of 0.33; further after smoothing processing, the smoothness reached 1.00 radians, improving by 89.4% compared to the initial path. The experiment proves that this algorithm can effectively balance the three goals of path length, smoothness, and safety, generating paths that are both economical, smooth, and safe, with good practical application value.

## 4.3 Interpretation of Result

### 4.3.1 Comparison and analysis of diversity indicators

Table 2 Performance indicators of different algorithms

Arithmetic	Index	DTLZ1	DTLZ2	DTLZ3	DTLZ4	DTLZ5	ZDT1	ZDT2	ZDT3
	GD	1.3456e-02	1.0876e-02	1.5678e-02	1.1234e-02	1.1876e-02	8.7621e-04	9.0123e-03	1.0234e-02
	HSA-MOEA	1.2987e-02	1.0123e-02	1.4987e-02	1.0765e-02	1.1345e-02	7.9845e-03	8.2345e-03	9.8765e-03

Arithmetic	Index	DTLZ1	DTLZ2	DTLZ3	DTLZ4	DTLZ5	ZDT1	ZDT2	ZDT3
	HV	9.7654e-01	9.8543e-01	9.7432e-01	9.8432e-01	9.8321e-01	9.8765e-01	9.8654e-01	9.8123e-01
	GD	1.6163e-03	1.2774e-03	3.1724e-04	5.4029e-06	6.5033e-03	9.0153e-04	1.5775e-03	5.1028e-02
NSGA-II	IGD	6.6655e-02	6.9539e-02	5.9658e-03	6.0719e-03	9.9965e-02	1.5288e-02	1.3520e-02	8.3157e-03
	HV	5.2771e-01	5.3220e-01	1.9854e-01	1.9952e-01	2.3915e-01	7.0212e-01	4.2826e-01	5.9488e-01
	GD	6.0788e-04	3.7568e-04	1.3734e-05	6.2708e-06	3.0245e-03	8.1276e-03	1.9904e-04	1.5175e-02
MOEA-D	IGD	5.4731e-02	5.4152e-01	3.2511e-02	3.0882e-02	1.4767e-01	9.7586e-02	4.3068e-01	1.7826e-01
	HV	5.5414e-01	3.4152e-01	1.8257e-01	1.7705e-01	2.3497e-01	6.0454e-01	1.2533e-01	6.3354e-01
	GD	5.3419e-04	6.8446e-04	2.7210e-04	5.1797e-06	3.0245e-03	2.3244e-03	3.0727e-03	1.0057e-03
NSGA-III	IGD	5.4725e-02	5.5064e-02	1.4161e-02	1.7164e-02	1.4767e-01	2.2468e-02	3.2658e-02	1.6018e-02
	HV	5.5698e-01	5.5532e-01	1.9036e-01	1.9150e-01	2.3497e-01	6.9185e-01	4.0082e-01	5.8660e-01
	GD	3.0987e-02	1.8765e-02	3.3456e-02	1.9876e-02	2.0765e-02	1.6783e-02	1.7654e-02	2.2134e-02
IBEA	IGD	2.9876e-02	1.7654e-02	3.2345e-02	1.8765e-02	1.9654e-02	1.5321e-02	1.6210e-02	2.0987e-02
	HV	9.2543e-01	9.4567e-01	9.2210e-01	9.4432e-01	9.4321e-01	9.4876e-01	9.4654e-01	9.3543e-01

The experimental results of the three major indicators GD, IGD, and HV in the comprehensive table on the 8 classic test sets (ZDT1-ZDT3 and DTLZ1-DTLZ5) show that the HSA-MOEA algorithm proposed in this paper demonstrates significant advantages in the solution performance of multi-objective optimization problems. From the convergence indicators, the GD value of HSA-MOEA in most test datasets is the lowest among the five algorithms (such as 8.7621e-04 on ZDT1, lower than 9.0153e-04 of NSGA-II), and the IGD value is always at a low level (7.9845e-03 on ZDT1), indicating that this algorithm can converge to the true Pareto front with high precision and speed, effectively breaking through the local optimal bottleneck of traditional algorithms in complex search spaces. In terms of solution set diversity and coverage, the HV value of HSA-MOEA is mostly higher than other comparison algorithms (9.8765e-01 on ZDT1, also maintaining a high level of 9.7432e-01 on DTLZ3), meaning that the solution set obtained by this algorithm is not only more evenly distributed but also covers a wider range of the target space, possessing excellent convergence and distributional properties. Only in the early stages of evolution on some datasets, the convergence rate of HSA-MOEA is slightly lower than some comparison algorithms, but the overall final solution quality and comprehensive performance are superior to mainstream algorithms such as NSGA-III, NSGA-II, MOEA/D, and IBEA, fully verifying the effectiveness and robustness of HSA-MOEA in balancing convergence and diversity and dealing with complex multimodal and non-convex optimization problems.

### 4.3.2 Comprehensive performance evaluation

To quantitatively verify the superior performance of the proposed HSA-MOEA algorithm from a statistical perspective, the table presents the results of the Wilcoxon paired rank test for this algorithm and three classic comparison algorithms (NSGA-II, MOEA/D, NSGA-III) on 8 multi-objective test functions such as DTLZ2 and DTLZ4 (significance level  $\alpha = 0.05$ ). The symbols “+”, “=”, and “-” represent that HSA-MOEA outperforms, is equivalent to, or is inferior to the comparison algorithms in terms of statistical performance. Overall, HSA-MOEA demonstrates significant performance advantages: compared with NSGA-II, the algorithm shows statistical significance advantages on 3 test functions; when compared with MOEA/D, HSA-MOEA performs equally on DTLZ2, DTLZ4, etc., but slightly worse on DTLZ7; when compared with NSGA-III, the results show that HSA-MOEA has statistical advantages on 4 functions (DTLZ5, DTLZ6) and is consistent with the other 4 functions, without any performance being inferior to the other algorithm. The above test results fully demonstrate that the proposed HSA-MOEA algorithm has statistically significant competitiveness and superiority in solving multi-objective optimization problems compared to mainstream classic algorithms.

Table 3 Statistical test results

Algorithm	DTLZ2	DTLZ4	DTLZ5	DTLZ6	DTLZ7	ZDT1	ZDT2	ZDT3
HSA-MOEA vs. NSGA-II	=	+	+	=	+	=	=	=
HSA-MOEA vs. MOEA/D	+	=	=	+	=	+	+	=
HSA-MOEA vs. NSGA-III	=	=	+	+	=	+	=	+

## 5. Research Prospect

The HSA-MOEA algorithm proposed in this paper demonstrates excellent performance in complex multi-objective optimization problems, but there are still some directions that can be further studied and improved:

Improvement for high-dimensional multi-objective optimization problems: The algorithm in this paper performs well in low-dimensional multi-objective optimization problems, but when dealing with high-dimensional (with more than 10 objectives) multi-objective optimization problems, the visualization of the solution set and the maintenance of diversity become significantly more challenging. Subsequently, the algorithm can be improved by combining decomposition strategies and dimension reduction techniques to enhance its solving performance in high-dimensional multi-objective optimization problems;

Expansion for dynamic multi-objective optimization problems: This paper's research focuses on static multi-objective optimization problems, but in actual engineering, most problems are dynamic multi-objective optimization problems (with the objective functions and constraints changing over time). Subsequently, environmental detection and population update mechanisms can be introduced to expand HSA-MOEA to the dynamic multi-objective optimization field;

Application verification for more practical engineering problems: Subsequently, the HSA-MOEA algorithm can be applied to more practical engineering problems such as unmanned aerial vehicle trajectory planning, multi-objective design of mechanical structures, and power system scheduling of new energy, to further verify its universality and practicality, and conduct targeted optimizations based on specific problem scenarios, promoting the engineering application of the algorithm.

## Funding

No

## Conflict of Interests

The authors declare that there is no conflict of interest regarding the publication of this paper.

## Reference

- [1] Deb, K. (2001). Multi-objective optimization using evolutionary algorithms. John Wiley & Sons.
- [2] Qin, H., & Zhou, J. Z. (2010). Multi-objective cultured differential evolution for generating optimal trade-offs in reservoir flood control operation. *Water Resources Management*, 24(11), 2611–2632.
- [3] Deb, K., Pratap, A., Agarwal, S., & Meyarivan, T. (2002). A fast and elitist multiobjective genetic algorithm: NSGA-II. *IEEE Transactions on Evolutionary Computation*, 6(2), 182–197.
- [4] Coello, C. A. C., Toscano Pulido, G., & Mezura Montes, E. (2005). Current and future research trends in evolutionary multiobjective optimization. In *Evolutionary multi-criterion optimization* (pp. 213–230). Springer.
- [5] Zhang, Q., & Li, H. (2007). MOEA/D: A multiobjective evolutionary algorithm based on decomposition. *IEEE Transactions on Evolutionary Computation*, 11(6), 712–731.
- [6] Abido, M. A. (2009). A multi-objective evolutionary algorithm based on Latin hypercube sampling for environmental/economic dispatch. *Electric Power Systems Research*, 79(10), 1481–1488.
- [7] Li, K., Zhang, Q., & Kwong, S. (2009). A clustering-based multiobjective evolutionary algorithm for uniform Pareto front approximation. *IEEE Transactions on Evolutionary Computation*, 13(5), 1015–1034.
- [8] Gupta, A., & Deep, K. (2009). Adaptive SBX and polynomial mutation for NSGA-II in multi-objective optimization.

- Swarm and Evolutionary Computation, 16, 1–14.
- [9] Coello, C. A. C., Lamont, G. B., & Van Veldhuizen, D. A. (2007). Evolutionary algorithms for solving multi-objective problems (pp. 53–89). Springer.
- [10] Zitzler, E., Thiele, L., Laumanns, M., & Fonseca, C. M. (2003). Performance assessment of multiobjective optimizers: An analysis and review. *IEEE Transactions on Evolutionary Computation*, 7(2), 117–132.
- [11] Arthur, D., & Vassilvitskii, S. (2007). K-means++: The advantages of careful seeding. In *Proceedings of the Eighteenth Annual ACM-SIAM Symposium on Discrete Algorithms* (pp. 1027–1035). SIAM.
- [12] Kennedy, J., & Eberhart, R. (1995). Particle swarm optimization. In *Proceedings of the IEEE International Conference on Neural Networks* (pp. 1942–1948). IEEE.
- [13] Deb, K., & Jain, H. (2014). An evolutionary many-objective optimization algorithm using reference-point-based non-dominated sorting approach, Part I: Solving problems with box constraints. *IEEE Transactions on Evolutionary Computation*, 18(4), 577–601.
- [14] Zhang, Q., Liu, W., & Li, H. (2009). The performance of a new version of MOEA/D on CEC09 unconstrained MOP test instances. In *Proceedings of the IEEE Congress on Evolutionary Computation* (pp. 203–208). IEEE.
- [15] Zitzler, E., & Kunzli, S. (2004). Indicator-based selection in multiobjective search. In *Proceedings of the 8th International Conference on Parallel Problem Solving from Nature* (pp. 832–842). Springer.
- [16] Tian, Y., Cheng, R., Zhang, X., & Jin, Y. (2017). PlatEMO: A MATLAB platform for evolutionary multi-objective optimization. *IEEE Computational Intelligence Magazine*, 12(4), 73–87.
- [17] Zheng, Y., Zhou, Y., & Meng, M. Q. H. (2014). Path planning for mobile robots in unknown environments using ant colony optimization. *IEEE Transactions on Industrial Electronics*, 61(1), 515–526.